Fluid–sediment interactions at Eastern Mediterranean mud volcanoes: a stable isotope study from ODP Leg 160

A. Dählmann*, G.J. de Lange

Utrecht University, Faculty of Earth Sciences, Department of Geochemistry, P.O. Box 80021, 3508 TA Utrecht, The Netherlands

Abstract

Pore fluids from two ODP sites at Eastern Mediterranean mud volcanoes have been analyzed for their Cl concentration and their $\delta^{18}O$ and δD isotopic composition. The Cl data span a wide range of concentrations, from extremely depleted with respect to seawater (as low as 60 mM) at the crest of Milano dome (site 970) to strongly enriched (up to 5.4 M) at Napoli dome (site 971). Chloride enrichment is known to be due to dissolving Messinian evaporites, whereas the source of the low-Cl fluid is deduced from stable isotope data presented here. The isotopic composition of the endmember fluid is found to be $+10\permil$ for $\delta^{18}O$ and $-32\permil$ for δD for low- as well as for high-Cl waters. From this signature it can be concluded that neither gas hydrates nor meteoric water play a significant role in the freshening of the pore water. Several other processes altering the $\delta^{18}O/\delta D$ composition of pore waters are discussed and considered to be of only negligible influence. The process characterizing the isotopic composition of the fluid is found to be clay mineral dehydration (mainly smectite–illite transformation), corresponding to a depth range of 3.5–7 km and an elevated temperature of about 120–165°C. A quantitative estimate shows that this reaction is capable of producing the observed extreme Cl depletion.
© 2003 Elsevier Science B.V. All rights reserved.

1. Introduction

Like other vent and seep structures, mud volcanoes can be considered as windows to their underlying, deep fluid source, providing insight into the origin of the fluid and mud mobilized. During active periods, the sediment is erupted along with a fluid phase (water and gas) and deposited on the ocean floor as breccia, building up the mud volcano. Fluids, however, are not only expelled during eruptive events. Since fluid flow is also caused by continuous processes, such as compaction-derived advection, it also proceeds during dormant periods. At depth, fluid–sediment interactions imprint the fluid chemistry and their distinct signature is brought to the surface sediments by the ascending fluid. The analysis of shallow pore fluids (tens of cm to hundreds of m below seafloor),

---

* Corresponding author. Tel.: +31-30-253-5037;
Fax: +31-30-253-5302.
    E-mail address: a.daehlmann@geo.uu.nl (A. Dählmann).

therefore, provides a key to constrain the reactions occurring at depth.

The signature of the ascending deep fluid is overprinted by reactions with the surrounding sediment on its flow path. Pore waters at shallower levels, therefore, have to be regarded as a mixture of connate water, deep fluid, and an additional supply of products from secondary alteration reactions. Apart from reactions with the surrounding mineral phases, the formation or dissociation of gas hydrates may significantly affect the pore water composition. Thus, the interpretation of pore water analyses is not always straightforward and only detailed discussions help to illuminate the various processes that might be involved.

In this paper we provide an overview of processes affecting chlorinity, $\delta^{18}O$ and δD values of pore waters, and present data from two mud volcanoes at the Mediterranean Ridge, sampled during ODP Leg 160 [1]. The most intriguing fact of this data set is the extreme depletion in chloride concentration in some of the cores. Based on a broader suite of analyses than was previously available [2], we discuss the imprint of various fluid–sediment interactions and the potential presence of gas hydrates on the fluid chemistry to better constrain the responsible processes for mud volcano-expelled fluids and their origin.

2. Mediterranean mud volcanoes

2.1. Tectonic and geological setting of the sample locations

The Mediterranean Ridge is a morphological high, built up by the accretionary wedge of the converging plates of Africa and Eurasia (Fig. 1A; see also [3]). The corresponding volcanic arc of this subduction zone is the Hellenic Arc, comprising the islands of Santorini and Milos. Numerous mud volcanoes have been identified by sidescan sonar techniques [4] and sediment and pore water samples have been collected during several expeditions [1,5–7]. Two main areas were studied, the Olimpi Mud Volcano field (OMV) and the Anaximander Mountains (AM).

In the OMV area, where the two ODP sites studied here have been drilled during Leg 160, the convergence rate is rather high (25 mm/a) and the accretionary prism extends over the entire width of the Mediterranean Sea, with the sediments thrusted upon the Libyan margin in the south and backthrusted upon the Cretan margin in the north (incipient continental collision [8]). Consequently, there is no trench at the (outer) deformation front. The so-called Hellenic Trench, north of the inner deformation front (backstop), is a fore-arc basin in tectonic terms. The OMV area lies about 150 km behind the (outer) deformation front and the volcanic activity is related to the backstop structure.

The two mud volcanoes studied here are Milano dome (ODP site 970) and Napoli dome (ODP site 971) (Fig. 1B). Both sites reveal interfingering of hemipelagic and mud breccia sediments, indicating episodic, extrusive mud flow [1,3]. From the age of clasts within the mud breccia it can be concluded that mud volcanism at OMV is active since more than 1 Ma [1,9].

The age and source depth of the mud matrix, however, remain unclear. Whereas several authors suggest a source depth of up to several km [10] and early to middle Miocene age [9], recent studies support a shallow source depth of < 2 km and early Miocene (Messinian) age [3,11].

2.2. Previous pore water studies

Sediments retrieved during ODP Leg 160 were gas-rich and massive degassing has been observed at atmospheric pressure onboard. Pore waters of sites 970 C and 970 D are characterized by extremely low Cl concentration and nearby cores sampled earlier showed increasing $\delta^{18}O$ values with depth [2]. These observations were related to gas hydrate dissociation during core recovery, in accordance with in situ p,T conditions that are within the gas hydrate stability field [2]. However, samples of gas hydrates have as yet only been found at mud volcanoes in the AM area [5]. Even though the two study areas have different tectonic settings, the geochemical evidence from the OMV area and the gas hydrate samples from the AM area (cf. Fig. 1) lead to the assump-
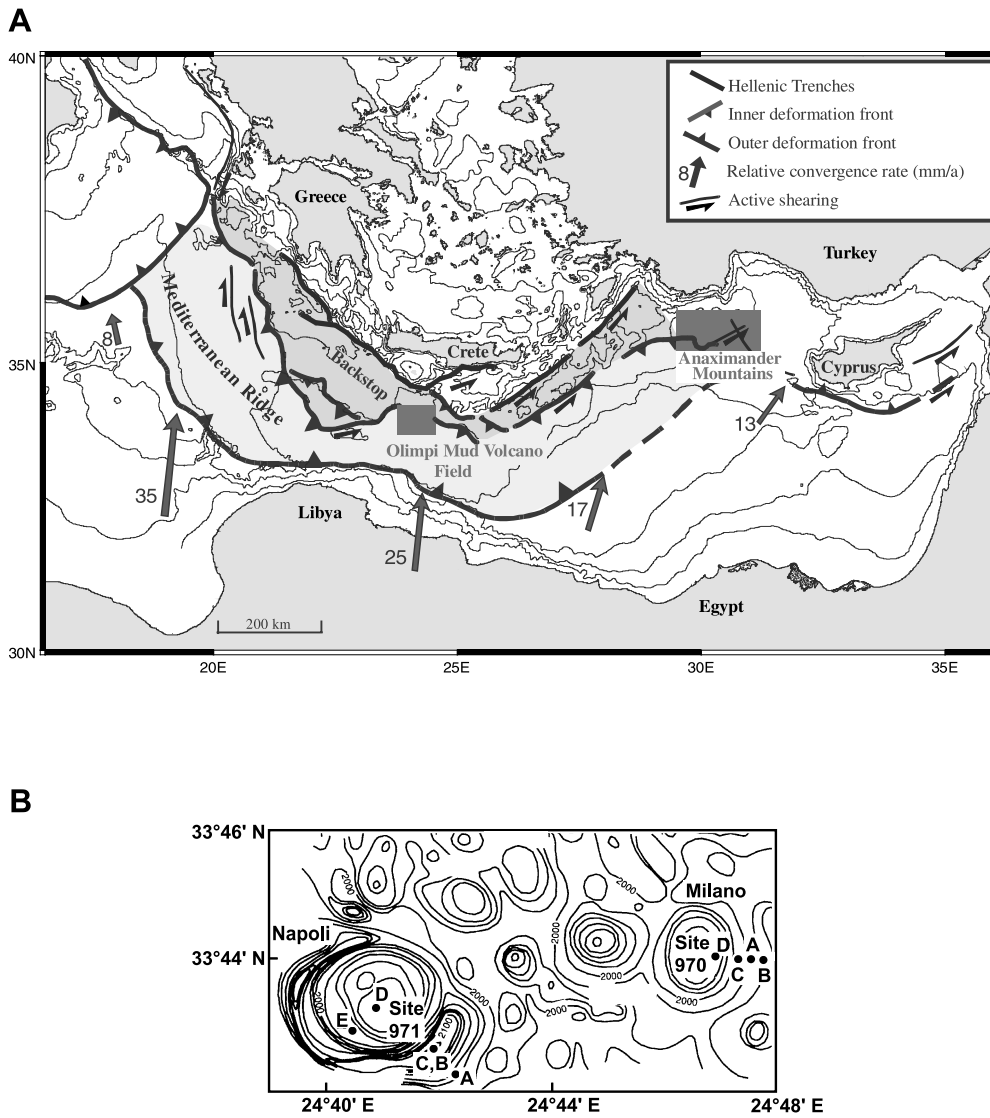
A

B

Fig. 1. (A) Map of the Eastern Mediterranean Sea with locations of the two main reseach areas, the Olimpi Mud Volcano field (OMV) and the Anaximander Mountains (AM) (map taken from [6]). (B) Detailed map of the two mud volcanoes Milano mud dome (site 970) and Napoli mud dome (site 971), situated in the OMV field and the specific positions of the drill sites (map taken from [1]).

tion that the presence of gas hydrate is a widespread phenomenon along the Mediterranean Ridge. Aloisi et al. [12] attributed rather high $\delta^{18}O$ signatures of carbonates of both areas (up to 7‰ PDB (PeeDee Belemnite), i.e. 38‰

SMOW (Standard Mean Ocean Water)) to the presence of gas hydrates, but they also concluded that further investigations are needed to evaluate the possible importance of diagenetic processes that might also increase the $\delta^{18}O$ of pore fluids.

Table 1
Cl concentration, oxygen and hydrogen isotopic composition of pore waters from Milano mud dome (site 970) and Napoli mud dome (site 971) with the positions of the sites and their respective water depths

	Depth (mbsf)	Cl (mM)	$\delta^{18}O$ (‰ SMOW)	δD (‰ SMOW)
Milano mud dome				
970 A	(33°44.194′N, 24°48.120′E; 2075.5 m)			
	5.90	606	1.6	n.a.
	8.95	607	1.6	9.7
	135.35	813	2.5	6.6
	144.95	844	2.6	7.8
	155.85	932	2.6	6.0
	165.53	1103	2.7	6.8
	173.85	1266	2.8	4.1
	184.55	1529	2.9	3.1
	194.50	1715	3.2	4.3
970 B	(33°44.214′N, 24°48.694′E; 2078.6 m)			
	5.90	794	2.1	9.2
	24.90	1159	2.3	8.7
	35.90	1373	2.6	6.5
	43.63	1537	2.7	6.9
970 C	(33°44.134′N, 24°47.457′E; 2036.9 m)			
	2.95	509	2.9	4.9
	7.52	369	4.7	−2.2
	9.70	350	5.2	−5.0
970 D	(33°44.042′N, 24°46.613′E; 1953.3 m)			
	1.27	183	6.9	−16.1
	12.10	202	7.1	−20.1
	23.10	236	8.2	−23.0
	30.71	61	9.0	−20.7
	41.80	88	9.0	−20.8
Napoli mud dome				
971 A	(33°42.190′N, 24°42.814′E; 2026.1 m)			
	4.40	678	1.6	9.8
	14.40	821	n.a.	n.a.
	20.90	956	2.0	10.8
	26.85	1169	2.1	9.0
	38.76	1648	2.5	5.2
	78.35	2864	n.a.	n.a.
	92.55	2977	3.1	−1.1
	103.65	3203	3.2	−1.7
971 B	(33°42.817′N, 24°42.108′E; 2140.9 m)			
	1.04	641	1.6	8.4
	8.10	810	1.8	8.5
	17.60	1047	2.2	7.9
	27.05	1402	2.5	5.6
	50.45	2862	4.3	−10.3
	59.51	2952	4.5	−11.5
	69.75	3400	4.9	−13.3
	98.88	4195	6.7	−20.9
	108.40	4082	6.7	−20.3
	118.00	4453	7.4	−23.0
	127.26	4331	7.4	−23.6
	138.74	3984	n.a.	n.a.
	148.53	3938	7.7	−22.3

Table 1 (*Continued*).

	Depth (mbsf)	Cl (mM)	$\delta^{18}O$ (‰ SMOW)	δD (‰ SMOW)
	167.70	3669	7.9	−22.8
	177.40	3468	8.0	−20.9
971 D	(33°43.437′N, 24°41.276′E; 1933.1 m)			
	1.35	4688	n.a.	n.a.
	2.85	5163	8.6	−23.4
	5.85	5408	9.0	−22.9
	10.85	5295	8.8	−23.0
	13.85	5348	n.a.	n.a.
	23.35	5354	n.a.	n.a.
	32.85	5365	9.0	−22.4
	37.85	5310	n.a.	n.a.
	45.35	5334	8.9	−22.4
971 E	(33°43.621′N, 24°40.839′E; 1943.6 m)			
	1.40	3535	4.7	−14.7
	2.90	4242	5.9	−18.3
	5.90	5010	7.8	−23.9
	8.90	5260	8.6	−24.9
	12.40	5158	8.5	−22.2
	16.80	5281	8.8	−22.5
	20.35	5128	8.4	−21.6
	27.81	5325	8.7	−23.7

Cl data are taken from [1]; n.a.: not analyzed.

3. Methods

Pore water sampling was done by ODP routine methods [1]. Chloride concentrations were determined immediately aboard R/V *Joides Resolution* by Mohr titration and potentiometric titration, respectively, with a precision of 0.2–0.4% [13,14]. Oxygen and hydrogen isotopic compositions were analyzed at Utrecht University by modified standard techniques. For $\delta^{18}O$ measurements 100 µl of the sample are equilibrated with 1.9 ml of a CO_2 standard. After two nights at 25°C a subsample of 1 ml is taken from the gas phase, the CO_2 is frozen out with liquid N_2 and its isotopic composition is determined by means of a stable isotope mass spectrometer (VG SIRA-24). Results are calculated considering isotopic composition of the standard as well as the fractionation in the CO_2/H_2CO_3 system and given relative to SMOW. All samples are measured at least in duplicate; precision is 0.1‰. δD is measured from a sample of 7 µl that is reduced to H_2 on uranium pellets at 680°C. The reduced hydrogen is then

desorbed and its isotopic composition is measured by means of a stable isotope mass spectrometer (VG SIRA-24). Results are given relative to SMOW. All samples are measured at least in duplicate; precision is $2‰$.

The different principles on which the isotopic measurements are based result in two different scales of the reported isotopic ratios. Whereas the oxygen isotopic values are based on the $H_2^{18}O$ activity (due to salt effects influencing the equilibrium with the vapor phase), the deuterium values are given in a concentration scale (because of a quantitative reduction at 680°C). For a discussion of the origin of the water, the $\delta^{18}O$ values have to be converted to the concentration scale, i.e. the isotopic signature of the free water has to be calculated. This is done by applying an empirical equation provided by Sofer and Gat [15]. However, the correction had only negligible effect ($\leq 0.1‰$, i.e. mostly far below the analytical precision), because the salt content of the mud volcano fluids is dominated by Na and Cl [1] that have only very little effect on the salt correction [15]. Nevertheless, we checked the possible effects by measuring a set of Mediterranean seawater with additions of NaCl, having total Cl concentrations from 0.6 to 4 M, after an equilibration time of 1 and 2 days, respectively. Again, no significant effect on the $\delta^{18}O$ value has been found, either with respect to the Cl concentration or to the equilibration time. Therefore, all results are reported without conversion.

4. Results

Each mud volcano is represented by four cores, namely 970 A, B, C, D for Milano and 971 A, B, D, E for Napoli mud dome. The pore waters show a large range in chlorinity (Table 1 and Fig. 2a,b). The most striking feature is the extreme difference of the crest samples between the two sites (closed symbols), showing a Cl concentration as low as 60 mM Cl at Milano dome (site 970 D) and as high as 5400 mM at Napoli dome (site 971 D). At the flank sites (open symbols), Cl is increasing with depth at both mud volcanoes. Core 971 B shows a particular Cl depth profile.

After reaching a maximum concentration of ~ 4.5 mM (at about 120 m below sea floor (mbsf)), the concentration is decreasing linearly with depth (down to ~ 3.5 M).

Despite their extreme difference in chlorinity, the depth profiles of the isotopic data of the crest samples are rather similar (Fig. 2c,d and Fig. 2e,f, respectively): The $\delta^{18}O$ and δD profiles mirror each other at both crest and flank samples, with $\delta^{18}O$ increasing and δD decreasing with depth.

All crest sites show very steep gradients in the upper 10 m of the sediment, whereas the flank sites show smoother transitions. At site 971, the deepest samples of the crest sites and of the flank site 971 B have similar absolute values in all parameters, whereas at site 970 the crest sites have much lower (Cl, δD) and higher ($\delta^{18}O$) values, respectively.

5. Discussion

We first discuss the possible imprint of Messinian evaporites on chlorinity profiles and the isotopic values (Section 5.1) as well as the effects of diagenetic reactions with various sedimentary compounds (Section 5.2). Subsequently, we discuss processes causing pore water freshening and their contribution to the pore water isotopic composition (Section 5.3) and, finally, quantitative aspects of the pore fluid freshening are considered (Section 5.4).

5.1. Imprint of Messinian evaporites

In the Mediterranean, Messinian evaporites are ubiquitously underlaying the subsurface sediments. They form a massive layer of variable thickness (up to more than 1000 m in the deepest parts of basins) that is found widespread and can usually be recognized as a distinct reflector in seismic profiles. The onset of mud volcanism at the Mediterranean Ridge has been assigned to an initial break of the evaporitic seal due to continued backthrusting of the accretionary wedge, allowing the overpressured fluid to escape [16]. The high salinity found in most of the pore water samples (Fig. 2a,b) is caused by the continuous
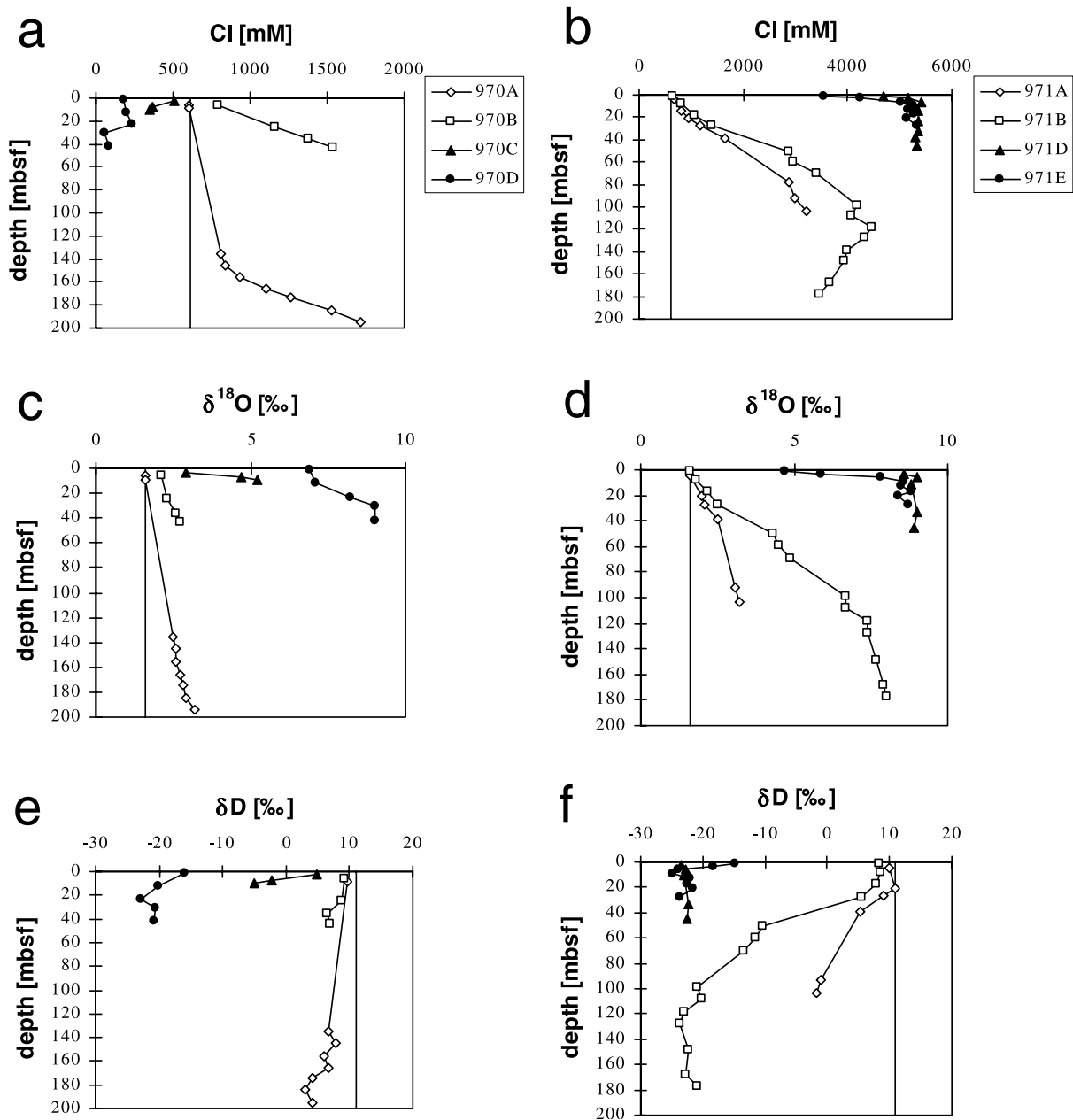
Milano dome

Napoli dome

Fig. 2. Cl concentration, oxygen and hydrogen isotopic composition of all sites at Milano mud dome (site 970) and Napoli mud dome (site 971). Isotopic data are given relative to SMOW. Closed symbols are crest sites, open symbols are flank sites. Note the scale difference between Cl plots of sites 970 and 971. Straight lines represent background compositions (609 mM Cl; +1.6‰ $\delta^{18}O$; +11‰ δD; sites 963 and 964; GdL, unpublished data).

dissolution of the evaporitic layer or by upward diffusion of deep brines.

At Napoli dome (site 971), the Cl concentration is generally enriched compared to seawater and reaches values of > 3 M over the whole sampled depth of the crest sites as well as in the deeper sediment (> 40 m) of the flank sites. At Milano dome (site 970), however, the distribution of Cl concentrations shows a high spatial heterogeneity, with depletion (as low as 60 mM) in the crest samples and enrichment (up to 1700 mM) at the flanks. Compared to the flank samples at Napoli dome the salinity at the flanks of Milano dome is much lower.

The shape of the Cl profile of core 971 B (Napoli dome) might be related to horizontal faults that occur within the mud breccia and serve as conduits for the high-Cl fluids advecting at ~ 120 m depth within the mud volcano. This lateral inflow results in an increased Cl concentration at this horizon and decreasing concentrations with distance to its depth. Another possible explanation of this Cl depth profile is to assume an admixture of a low-Cl fluid from below the sampling depth (see Section 5.3).

Whereas the simple dissolution of chloride salts by any unsaturated solution would increase the Cl concentration but leave the isotopic values unchanged, a possible contribution of residual brines is expected to cause an enrichment in both ^{18}O and D [17] (Table 2). However, the observed δD values are depleted and a δ^{18}O value of about 2‰ for relict Mediterranean brines [18] is too close to the background value of 1.6‰ for Mediterranean seawater [19] to alter the isotopic composition significantly.

5.2. Contributions of other sedimentary components

Several sedimentary components have δ^{18}O and δD values that differ significantly from the pore water composition and may, therefore, alter its isotopic composition by diagenetic reactions.

Marine carbonates and biogenic silica have relatively high δ^{18}O values of 27–38‰ SMOW (i.e. -4 to $+7$‰ PDB) [20]. Therefore, they may increase the δ^{18}O values of the pore water when a

recrystallization takes place at a temperature higher than their formation temperature. In the ODP cores, carbonates make up about 20% of the mud breccia and could therefore partly contribute to the high δ^{18}O values in the pore water, whereas the biogenic silica component is too small [1] to have an influence on the pore water δ^{18}O signature. Recrystallization of both minerals would, however, not change the δD (Table 2).

Tephra layers have been found at both ODP sites in the uppermost sedimentary layer [1] and can be found in many cores of the OMV area [21]. Their alteration would increase the δ^{18}O of the fluid if the reaction temperature is high, whereas below 300°C the effect is minor or even opposite, because ^{18}O is taken up by minerals during low-temperature alteration [22,23] (Table 2). Because temperatures at the fluid source depth are supposed to be moderate [24], high-temperature alteration can be excluded as a potential source of high δ^{18}O values. Furthermore, both high- and low-temperature alteration lead to an increase of δD in the fluid, as during hydration the lighter isotope is preferentially incorporated into secondary minerals [22,25] (Table 2). In constrast, a decrease is observed.

Kaolinite makes up about 20% of the clay mineral fraction of the mud breccia [26] and water in equilibrium with kaolinite has been found to have

Table 2
Synopsis of processes potentially occurring at the source depth of the mud volcano fluids and during the fluid ascent, with their respective imprints on pore water Cl concentration, δ^{18}O, and δD values

	Cl	δ^{18}O	δD
Messinian residual brine input	+	+	+
Carbonate recrystallization	o	+	o
Biogenic opal recrystallization	−	+	o
Ash particle alteration (low/high temp.)	o	−/+	+
Kaolinite–fluid interaction	o	+	−
Gas hydrate dissociation	−	+	+
Anaerobic methane oxidation	−	o	−
Meteoric water input	−	−	−
Clay membrane ion filtration	−	−	−
Clay mineral dehydration	−	+	−

Trends are given by '−' (decrease), '+' (increase), and 'o' (no change), respectively.
For references see text (Section 5).

an isotopic signature of +8 to +18‰ in $\delta^{18}O$ and −30 to −55‰ in δD [25,27] (Table 2). Exchange reactions of the pore fluid with this mineral will therefore alter the fluid composition in the way it is observed. However, the influence is minor compared to smectite (with an abundance of about 80%) and, additionally, cannot be distinguished from interactions with smectite because of the same isotopic signature of both processes.

5.3. Processes causing pore water freshening and their contributions to the $\delta^{18}O$ and δD pore water isotopic composition

Reduced pore water salinities have been reported for a number of sites and have been attributed to gas hydrate dissociation, meteoric water input, clay membrane ion filtration, and clay mineral dehydration, respectively (for references see the specific parts in the following text). Although all of these processes reduce the pore water salinity, their effect on the pore water (H_2O) oxygen and hydrogen isotopic composition is different. In the following we summarize the processes with their respective effects and give an overview in Table 2.

Fig. 3a shows the correlation between Cl concentration and $\delta^{18}O$ for all cores analyzed. Apart from two cores (970 C and D) and the lowermost samples of site 971 B, all data fit to one Cl–$\delta^{18}O$ correlation with increasing Cl for increasing $\delta^{18}O$ ($r^2 = 0.95$). The cores 970 C and D show decreasing Cl concentration for increasing $\delta^{18}O$ ($r^2 = 0.92$), with a total decrease of 400 mM Cl and an increase of 6‰ in $\delta^{18}O$.

The Cl profile of core 971 B (Fig. 2b) is retrieved in the $\delta^{18}O$/Cl plot (Fig. 3a), too. Whereas the upper samples of this core plot within the general trendline for evaporite-influenced pore waters, the lowermost three samples plot towards the low-Cl fluids of cores 970 C and D. The observed trend is also reflected in the δD/Cl plot (Fig. 3b), where the lowermost seven samples plot below the regression line. For site 971 B we can therefore conclude that the Cl profile is caused by an admixture of a low-Cl fluid from below the sampling depth carrying the isotopic signature of the supposed deep fluid.
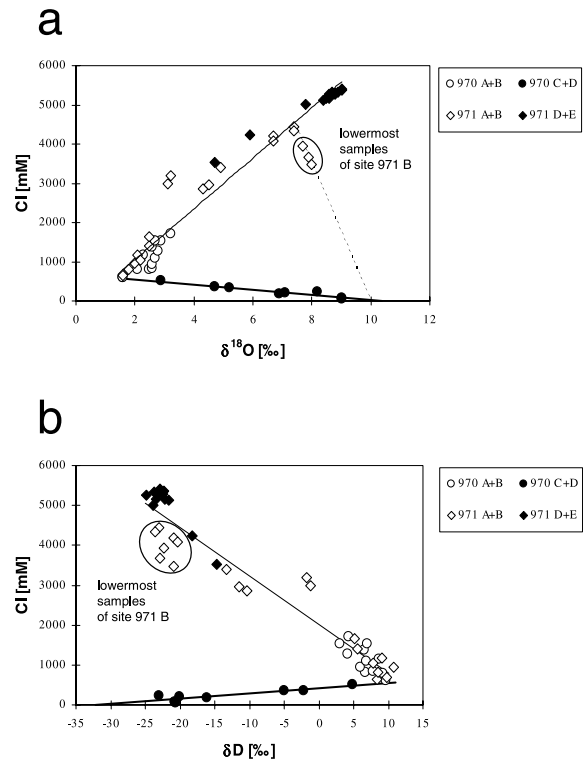
Fig. 3. Correlation of $\delta^{18}O$ (panel a) and δD (panel b) with Cl for all cores sampled at Milano and Napoli mud volcanoes. Crest sites are given as closed symbols and flank sites are given as open symbols. (a) The thick line represents the regression line for sites 970 C and D exibiting Cl depletion ($r^2 = 0.92$), giving an endmember composition of +10‰ $\delta^{18}O$ (at 0 mM Cl). The thin regression line is for all other sites, excluding the three lowermost samples of site 971 B ($r^2 = 0.95$). The dashed line indicates the trend from a high-Cl-dominated fluid towards a low-Cl-dominated fluid described by the three lowermost samples of site 971 B, leading towards the same $\delta^{18}O$ endmember signature. (b) The thick line represents the regression line for sites 970 C and D ($r^2 = 0.82$), giving an endmember composition of −32‰ δD (at 0 mM Cl). The thin regression line is for all other sites ($r^2 = 0.95$), also including the seven lowermost samples of site 971 B.

From Fig. 3 it becomes evident that the deep fluid is characterized by a low Cl concentration as well as a high $\delta^{18}O$ and a low δD value at both mud volcanoes. The secondary imprint of dissolved salts does not essentially alter the isotopic signature of the resulting mixed fluid, as has been discussed in Section 5.1.

We calculate the $\delta^{18}O$ endmember composition

of the low-Cl deep fluid by a linear extrapolation of the isotopic value towards zero chlorinity (Fig. 3a). The δD endmember can likewise be obtained from a plot of δD against Cl (Fig. 3b). The potential deep fluid is then characterized by a highly positive $\delta^{18}O$ value (+10‰) and a highly negative δD value (−32‰).

5.3.1. Gas hydrate dissociation

The decrease of Cl in pore waters as an artifact due to gas hydrate dissociation during core recovery is a well known phenomenon in subduction zone settings and has been observed in many cases (e.g. [28–31]). It is coupled with an increase in $\delta^{18}O$ and δD of the diluted pore water, since gas hydrates do not only exclude Cl from their lattice structure but also preferentially incorporate the heavier isotopes of O and H in their cage water. Dissociation of gas hydrates, therefore, results in positive trends for both $\delta^{18}O$ and δD towards the isotopic composition of natural gas hydrate. The latter has been obtained from values for dissociated hydrate samples corrected for any impurities from the surrounding pore water (+2.4 to +3.5‰ for $\delta^{18}O$ [32–36] and about +22‰ for δD [33]).

Decreasing Cl concentrations with increasing $\delta^{18}O$ values (Fig. 3a) resemble the results from ODP Leg 164 (Blake Ridge), where negative Cl and positive $\delta^{18}O$ anomalies have been attributed to ex situ dissolution of gas hydrates [29]. Although the largest Cl anomalies observed at Blake Ridge (ΔCl = 400 and 200 mM, respectively) are in the order of what is observed at the Mediterranean mud volcanoes, the $\delta^{18}O$ increases at Blake Ridge are only +0.7‰ and +0.4‰, respectively. Taking into account that the maximum $\delta^{18}O$ value of gas hydrate water hitherto observed is 3.5‰ [35], it is obvious that the large increase in $\delta^{18}O$ at the Mediterranean mud volcanoes has a different source than the release of ^{18}O-enriched hydrate water.

A $\delta^{18}O$/δD correlation (Fig. 4) can help to further support this interpretation. In contrast to the correlation of $\delta^{18}O$ with Cl, all data fit to one correlation line ($r^2 = 0.93$) and samples with low Cl values (closed circles) are spread all over the data set, suggesting that the Cl concentration is
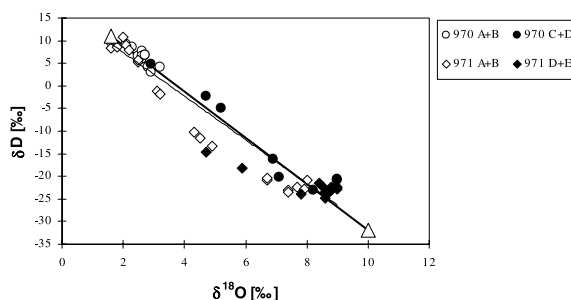

Fig. 4. Correlation of $\delta^{18}O$ with δD for all cores sampled at Milano and Napoli mud volcanoes. Solid symbols represent crest cores, open symbols flank cores. The thick line represents the mixing line between the supposed endmember values (large triangles) of background pore water (see Fig. 2) and deep fluid (see Fig. 3) and is almost identical with the regression line of all data (thin line; $r^2 = 0.93$).

not directly related to the isotopic composition of the pore waters. The good correlation indicates that both isotopes are altered by the same process, leading to an increase of $\delta^{18}O$ and a decrease of δD. Since the dissolution of gas hydrates would lead to a simultaneous increase of both isotopes, it is clear that gas hydrates cannot play a major role in the observed $\delta^{18}O$ and δD shifts.

5.3.2. Anaerobic methane oxidation

Although the presence of gas hydrate cannot be proven by the isotopic data, high methane concentrations (up to 100% of the total gas) have been measured in the pore water [1]. Since bacterial methane is highly depleted in D (δD ca. −200‰ [37,38]), anaerobic methane oxidation ($CH_4 + SO_4^{2-} \Leftrightarrow HS^- + HCO_3^- + H_2O$) generates water that is rather light in δD. However, the in situ concentration of methane is negligible compared to the total 'concentration' of H_2O in the pore water (55 M), so that even a very large flux of methane will result in only a marginal shift in δD.

5.3.3. Meteoric water input

The relationship between $\delta^{18}O$ and δD in meteoric water is described for the Mediterranean with a specific meteoric water line (δD = $8\delta^{18}O$ +22‰ [39]). As the lighter isotopes are evaporated more effectively, the corresponding meteoric water is lighter in both isotopes. An input of meteoric
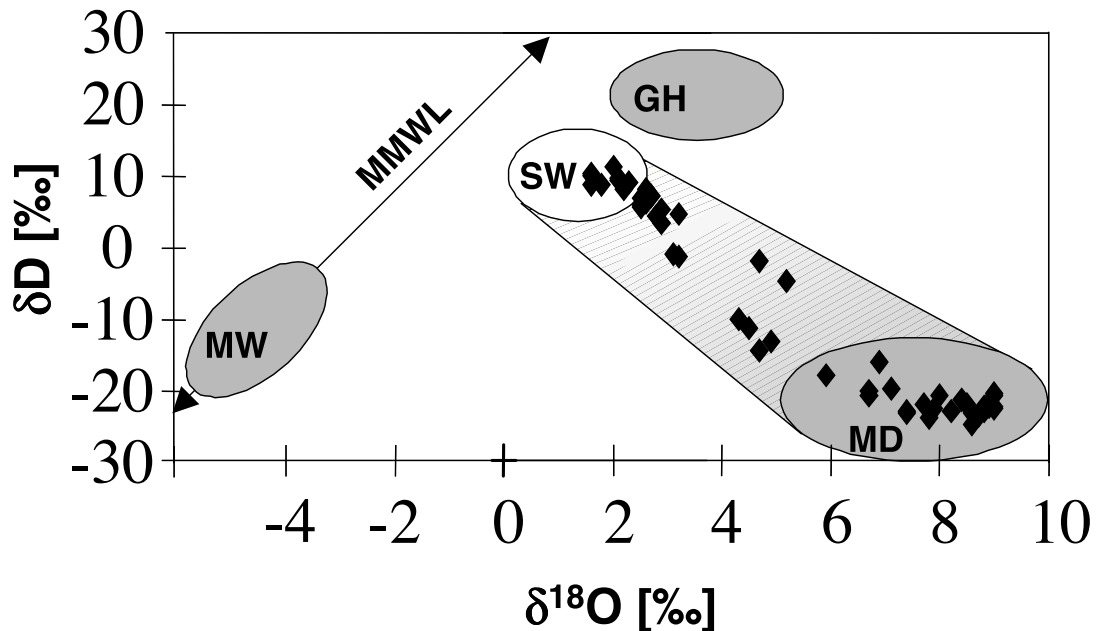
Fig. 5. $\delta^{18}O$ and δD data for all samples from Milano and Napoli mud volcanoes (sites 970 and 971) with a schematic overview of processes potentially reducing the fluid salinity (for references, see text Section 5.3). SW, Mediterranean seawater (1.6‰ $\delta^{18}O$; +11‰ δD; see Fig. 2); MMWL, Mediterranean meteoric water line ($\delta D = 8\delta^{18}O +22‰$) with meteoric water (MW) that corresponds to the SW value; GH, gas hydrate ($\delta^{18}O$ +3‰, δD +20‰); MD, clay mineral dehydration (trend leading towards $\delta^{18}O$ +20‰, δD −70‰). Please note that this is a sketch only and no exact data should be read from it.

water would, therefore, result in a negative shift of $\delta^{18}O$ and δD values towards the meteoric water line. Since no samples have positive δD values, i.e. do not plot towards the meteoric water line, there is no evidence for a fresh-water influence.

5.3.4. Clay membrane ion filtration

The ability of clay minerals to 'filter' specific ions out of the pore water, clay membrane ion filtration, is dependent on the ion charge and its diameter as well as the mineralogy of the clay and its respective cation exchange capacity. Kastner et al. [40] stated that this process may be a more important process lowering the Cl concentration than previously assumed. The filtration leads to a decrease in Cl and the heavier isotopes (^{18}O, D) in the fluid that passed the clay layer [41]. However, the possibility of clay membrane ion filtration is considered to be negligible, because the filtrate is expected to be depleted in ^{18}O (e.g. [41]), whereas an enrichment is observed. This is in agreement with data from the Barbados accretionary com-

plex discussed by Gieskes et al. [42], where this process was also dismissed.

5.3.5. Mineral dehydration

Due to the sediment load and the geothermal gradient, mineral dehydration takes place at a greater depth of the accretionary prism. Minerals release their structural water and are transformed into secondary minerals, thereby freshening the ambient pore water. The main reactions are smectite(S)–illite(I) transformation, opal dehydration, and deeper metamorphic reactions (e.g. [43]). The S–I transformation starts at about 60°C and is almost complete at about 160°C [40,44]. With increasing pressure and temperature the amount of water released from the clay interlayers increases. The S-dominated clay assemblage is thereby gradually transformed into an S/I assemblage and eventually, after having lost the last water interlayer, becomes an illitic clay [45]. The interlayer water of clay minerals is generally characterized by positive $\delta^{18}O$ and negative δD values.

Magaritz and Gat [20] report the general isotopic composition of the carbonate-free portion of oceanic sediments to be +11.5 to +28.5‰ in $\delta^{18}O$ and −55 to −87‰ in δD. During fluid–sediment interactions, the fluid-$\delta^{18}O$ will, therefore, increase, whereas its δD will decrease.

The most likely process to reduce pore water salinity and to explain the $\delta^{18}O$ and δD signature of the endmember fluid is mineral dehydration. Dehydration of opal and metamorphic reactions cannot contribute essentially to pore water freshening, because the Mediterranean sediments do not contain substantial amounts of opal [1] and the p,T conditions of the fluid source region are supposed to be relatively moderate [24]. Smectite, however, is highly abundant in the analyzed sediments (up to 80% of the clay mineral fraction [26]) and its transition to illite could take place to an extent that causes the observed large decrease in pore water chlorinity (Section 5.4). The endmember signature of +10‰ in $\delta^{18}O$ and −32‰ in δD can easily be achieved by the release of clay interlayer water. Assuming an isotopic composition of smectite of +17 to +23‰ in $\delta^{18}O$ and −35 to −55‰ in δD, respectively [46], and a fractionation of the water release of

10‰ at 150°C for both isotopes [25,46], the resulting fluid composition is +7 to +13‰ in $\delta^{18}O$ and −25 to −45‰ in δD, respectively. Thus, the observed values from the Mediterranean mud volcanoes perfectly fit into this range. The discussed processes with their respective imprint on the $\delta^{18}O$ and δD isotopic composition of the pore water and the observed data are summarized in Fig. 5.

Adapting a p,T diagram of [45] that illustrates the regions of the different water layer losses to the Mediterranean situation (water depth, bottom water temperature, geothermal gradient) reveals that the p,T conditions of smectite–illite transition lie in the range of 120–165°C and a corresponding depth of 3.5–6.8 kmbsf. This temperature range is in good agreement with the previously inferred source depth of the fluid and the geothermal gradient (5–7 km, 25°C/km [8,24]).

5.4. Quantitative aspects of smectite dehydration

To consider the amount of water that can potentially be released from a certain volume of sediment by clay mineral dehydration, we calculated three (closed system) scenarios (Table 3) with varying values for porosity, smectite content,

Table 3
Calculation of three (closed system) scenarios to estimate the amount of interlayer water that may be released and account for the pore water freshening

	Scenario 1 conservative	Scenario 2 intermediate	Scenario 3 maximum
Variable parameters			
Porosity	0.4	0.3	0.2
Smectite content of dry sediment (wt%)	40	45	50
Interlayer water content of smectite (wt%)	10	15	25
Calculated sediment parameters (wt% of wet sediment)			
Sediment content	77	83	90
Pore water content	23	17	10
Smectite content of dry sediment	31	37	45
Interlayer water content of smectite	3	6	11
Pore water dilution after release of interlayer water			
Dilution of initial pore water (%)	12	25	53
Cl concentration of diluted pore water (mM)	537	458	287

The variable parameters are based on literature data given in the text.
The dilution of the pore water and the Cl concentration of the diluted pore water, respectively, are calculated as follows: The dry sediment and initial pore water content are calculated from the porosity. The smectite content and the corresponding interlayer water content are determined from its proportion in the dry material and its water content, respectively. The produced amount of fresh water is then 'added' to the initial pore water content and the dilution factor as well as the diluted concentration are evaluated. The initial pore water concentration is assumed to be the same as Mediterranean bottom water (609 mM at sites 963 and 964 [1]).

and interlayer water content of the smectite. The assumed porosities are taken from the range of (modeled) data for the Barbados accretionary wedge [47]. The variation in the smectite water content is justified by the range given in the literature [25,43,44]. Analyses of the hydrous clay mineral content of mud breccia at sites 970 and 971 reveal a maximum content of smectite in the bulk sediment of 49% within the upper 200 m of the mud volcanoes [26]. Since there are no data available to predict the clay content of deeper strata, 50% is taken as a maximum percentage and the more conservative calculations are based on its incomplete dehydration. Whereas the sediment matrix does not seem to have undergone smectite–illite transition due to burial diagenesis [26,48], there is evidence that the fluids come from deeper strata than the adjacent solid mud phase [24]. Therefore, high amounts of smectite and small amounts of illite in the mud breccia do not contradict the conclusion of deep-seated smectite–illite transformation. The reaction products and released interlayer water are transported to the surface sediments by fluids originating from depths as great as the décollement (5–6 km [24]), where the reaction is thought to take place.

Using the above-mentioned literature data, our first scenario is based on a rather high porosity at depth of the accretionary prism (0.4), a smectite content that corresponds to 80% of the measured content in the mud breccia (40%), and a minimum estimate for the interlayer water content of the smectite (10%). These assumptions result in a conservative estimate of water release. While the second scenario uses intermediate assumptions, the third one gives a maximum of pore water dilution, assuming a rather low porosity (0.2), the maximum smectite content measured (50%), and a high interlayer water content of the smectite (25%). The way of calculating is described in the legend of Table 3.

Our results show that a pore water dilution of only 12% is achieved by considering the most conservative assumptions. The intermediate scenario gives a dilution of 25%, while the third scenario leads to a Cl depletion of 53%. The calculated range is in excellent agreement with compiled pore water data from various subduction zone settings (Barbados Ridge, Nankai Trough, Peru Margin), showing Cl dilutions of 10–40% related to smectite dehydration [40]. A maximum depletion of 55% was found in a mud pie near the Barbados accretionary complex. Modeling of pore water data from the Nankai wedge [43] leads to the conclusion that the majority of the Cl anomaly (30%) may be attributed to smectite–illite transition, even if the initial abundance of smectite is only moderate (10–15% of the bulk sediment). Morton and Land [49] modeled the salinity of connate water that is refreshed solely due to the release of smectite interlayer water and achieved a maximum depletion of about 75% (140 mM Cl).

To check the quality of our approach, we applied data of the Nankai wedge that have been modeled by Brown et al. using a two-dimensional numerical hydrologic model that couples fluid flow, solute transport, and a kinetic reaction model for smectite dehydration [43]. These authors found that the bulk of the observed maximum Cl reduction (110 mM) can be caused by S/I transition alone. Using their range of parameters (for porosity, smectite content, and interlayer water content), our calculation results in a pore water Cl concentration reduced by 25–110 mM. This is in good agreement with the results achieved with the numerical model and thus proves the overall good applicability of our approach.

The result of the above calculation gives the possible dilution that can be achieved within a given sediment volume (closed system approach). Certainly, the fluid expelled at a mud volcano does not only originate from the area it covers, but at these vent sites the dewatering of a larger area is focused. This concept implies that the dewatering takes place at a certain depth level and over a certain area of the accretionary prism, i.e. including lateral inflow of likewise diluted water masses, and that the depleted pore water is subsequently transported upwards, eventually being expelled at the mud volcano site.

To explain the observed Cl decrease by mineral dehydration, it can be estimated that a catchment area of less than eight times the mud volcanoes' surface would be sufficient (90% observed dilution/ > 12% calculated dilution = < 7.5). To assess

whether such a catchment area is reasonable we consider the abundance of mud volcanoes within the OMV field. From a map (e.g. [21]) it appears that this area is covered with mud volcanoes to about 5%. Assuming that the mud volcanoes alone account for the dewatering of the whole OMV field, the catchment area would be about 20 times the mud volcano surface area. The fluids are particularly kept back by the massive, ubiquitous layer of Messinian evaporites and are channeled where this cap is broken (e.g. by faulting). But even when considering disperse flow that may generally account for at least a third of the total flow in an accretionary prism [50], the potential catchment area being dehydrated at depth is about 13 times the area of known mud volcanoes.

As the calculations above revealed that an area not larger than eight times is needed, it is clear that the area under consideration is large enough to release a sufficient amount of water to explain the observed freshening of the pore water. Thus, smectite–illite transition is not only a plausible reaction in terms of the geological conditions required (smectite abundance, p, T) and the isotopic compositions observed ($\delta^{18}O$, δD), but can also satisfactorily explain the observed Cl depletion quantitatively.

6. Conclusion

The $\delta^{18}O$ and δD isotopic composition and the Cl concentration of pore fluids from two Eastern Mediterranean mud volcanoes can be described by a mixture of seawater with a high-$\delta^{18}O$ (+10‰), low-δD (−32‰) deep fluid. At Milano dome (ODP site 970), the advecting deep fluid is characterized by extremely low Cl concentrations (as low as 60 mM Cl), whereas at Napoli dome (site 971) this signature is heavily overprinted by dissolved Messinian evaporites (up to 5.4 M Cl). Our stable isotope analyses of the pore waters give evidence that the Cl concentration is not directly related to the isotopic composition of the pore water, i.e. both low- and high-Cl fluids exhibit the same isotopic endmember.

It is shown that the mud volcanoes do not harbor significant amounts of gas hydrate and the

input of meteoric water could likewise be rejected as a source for pore water dilution. Clay membrane ion filtration is likely to be negligible. Therefore, the main process characterizing the fluid's isotopic composition is clay mineral dehydration. The discussed processes with their respective imprint on the $\delta^{18}O$ and δD isotopic composition of the pore water and the observed data are summarized in Fig. 5. A quantitative estimate revealed that smectite–illite transformation is capable of producing even the observed extreme Cl depletion.

Our detailed study of several pore water parameters demonstrates that only an extended data set including Cl, $\delta^{18}O$, and δD enables one to distinguish between the various possible processes causing pore water freshening.

References

[1] K.-C. Emeis, A.H.F. Robertson, C. Richter et al. (Eds.), Proc. ODP Init. Repts. 160 (1998) 972 pp.

[2] G.J. De Lange, H.-J. Brumsack, Pore-water indications for the occurrence of gas hydrates in Eastern Mediterranean mud dome structures, in: A.H.F. Robertson, K.-C. Emeis, C. Richter, A. Camerlenghi (Eds.), Proc. ODP Sci. Res. 160 (1998) 569–574.

[3] A.H.F. Robertson, A. Kopf, Tectonic setting and processes of mud volcanism on the Mediterranean Ridge accretionary complex: Evidence from Leg 160, in: A.H.F. Robertson, K.-C. Emeis, C. Richter, A. Camerlenghi (Eds.), Proc. ODP Sci. Res. 160 (1998) 665–680.

[4] N. Fusi, N.H. Kenyon, Distribution of mud diapirism and other geological structures from long-range sidescan

sonar (GLORIA) data, in the Eastern Mediterranean Sea, Mar. Geol. 132 (1996) 21–38.

[5] J.M. Woodside, M.K. Ivanov, A.F. Limonov, Shipboard Scientists of the ANAXIPROBE expeditions, Shallow gas and gas hydrates in the Anaximander Mountains region, eastern Mediterranean Sea, in: J.-P. Henriet, J. Mienert (Eds.), Gas Hydrates - Relevance to World Margin Stability and Climate Change, Geol. Soc. London Spec. Publ. 137 (1998) 177–193.

[6] MEDINAUT/MEDINETH Shipboard Scientific Parties, Linking Mediterranean brine pools and mud volcanism, EOS Trans. AGU 81 (2000) 625–632.

[7] M.B. Cita, M.K. Ivanov, J.M. Woodside (Eds.), The Mediterranean Ridge Diapiric Belt, Mar. Geol. 132 (1996) 271 pp.

[8] A. Camerlenghi, M.B. Cita, B. Della Vedova, N. Fusi, L. Mirabile, G. Pellis, Geophysical evidence of mud diapirism on the Mediterranean Ridge accretionary complex, Mar. Geophys. Res. 17 (1995) 115–141.

[9] I. Premoli Silva, E. Erba, S. Spezzaferri, M.B. Cita, Age variation in the source of the diapiric mud breccia along and across the axis of the Mediterranean Ridge Accretionary Complex, Mar. Geol. 132 (1996) 175–202.

[10] H.-M. Schulz, K.-C. Emeis, N. Volkmann, Organic carbon provenance and maturity in the mud breccia from the Napoli mud volcano: Indicators of origin and burial depth, Earth Planet. Sci. Lett. 147 (1997) 141–151.

[11] A. Kopf, A.H.F. Robertson, N. Volkmann, Origin of mud breccia from the Mediterranean Ridge accretionary complex based on evidence of the maturity of organic matter and related petrographic and regional tectonic evidence, Mar. Geol. 166 (2000) 65–82.

[12] G. Aloisi, C. Pierre, J.-M. Rouchy, J.-P. Foucher, J. Woodside, MEDINAUT Scientific Party, Methane-related authigenic carbonates of eastern Mediterranean Sea mud volcanoes and their possible relation to gas hydrate destabilisation, Earth Planet. Sci. Lett. 184 (2000) 321–338.

[13] J.M. Gieskes, T. Gamo, H. Brumsack, Chemical Methods for Interstitial Water Analysis aboard Joides Resolution, ODP Technical Note 15, Ocean Drilling Program, College Station, TX, 1991. (can be downloaded from http://www-odp.tamu.edu/publications/).

[14] G.J. De Lange, Shipboard routine and pressure-filtration system for pore-water extraction from suboxic sediments, Mar. Geol. 109 (1992) 77–81.

[15] Z. Sofer, J.R. Gat, Activities and concentrations of oxygen-18 in concentrated aqueous salt solutions: Analytical and geophysical implications, Earth Planet. Sci. Lett. 15 (1972) 232–238.

[16] A. Robertson, Ocean Drilling Program Leg 160 Scientific Party, Mud volcanism on the Mediterranean Ridge: Initial results of Ocean Drilling Program Leg 160, Geology 24 (1996) 239–242.

[17] J.R. Gat, Oxygen and hydrogen isotopes in the hydrologic cycle, Annu. Rev. Earth Planet. Sci. 24 (1996) 225–262.

[18] B. Stenni, A. Longinelli, Stable isotope study of water, gypsum and carbonate samples from the Bannock and Tyro Basins, eastern Mediterranean, Mar. Chem. 31 (1990) 123–135.

[19] C. Pierre, The oxygen and carbon isotope distribution in the Mediterranean water masses, Mar. Geol. 153 (1999) 41–55.

[20] M. Magaritz, J.R. Gat, Review of the natural abundance of hydrogen and oxygen isotopes, in: J.R. Gat, R. Gonfiantini (Eds.), Stable Isotope Hydrology - Deuterium and Oxygen-18 in the Water Cycle, Technical Reports Series 210, International Atomic Energy Agency, Vienna, 1981, pp. 85–102.

[21] M.B. Cita, E. Erba, R. Lucchi, M. Pott, R. van der Meer, L. Nieto, Stratigraphy and sedimentation in the Mediterranean Ridge diapiric belt, Mar. Geol. 132 (1996) 131–150.

[22] W.C. Shanks, J.K. Böhlke, R.R. Seal, Stable isotopes in mid-ocean ridge hydrothermal systems: Interactions between fluids, minerals, and organisms, in: S.E. Humphris, R.A. Zierenberg, L.S. Mullineaux, R.E. Thomson (Eds.), Seafloor Hydrothermal Systems, Geophysical Monograph 91, AGU, Washington, DC, 1995, pp. 194–221.

[23] J.M. Gieskes, J.R. Lawrence, Alteration of volcanic matter in deep sea sediments: evidence from the chemical composition of interstitial waters from deep sea drilling corres, Geochim. Cosmochim. Acta 45 (1981) 1687–1703.

[24] A. Deyhle, A. Kopf, Deep fluids and ancient pore waters at the backstop: Stable isotope systematics (B, C, O) of mud volcano deposits on the Mediterranean Ridge accretionary wedge, Geology 29 (2001) 1031–1034.

[25] S.M.F. Sheppard, H.A. Gilg, Stable isotope geochemistry of clay minerals, Clay Miner. 31 (1996) 1–24.

[26] M.J. Jurado-Rodríguez, F. Martínez-Ruiz, Some clues about the Napoli and Milano mud volcanoes from an integrated log-core approach, in: A.H.F. Robertson, K.-C. Emeis, C. Richter, A. Camerlenghi (Eds.), Proc. ODP Sci. Res. 160 (1998) 607–624.

[27] A. Bechtel, S.M. Savin, S. Hoernes, Oxygen and hydrogen isotopic composition of clay minerals of the Baloul Formation in the region of the Bou Grine zinc-lead ore deposit (Tunisia): evidence for fluid-rock interaction in the vicinity of salt dome cap rock, Chem. Geol. 156 (1999) 191–207.

[28] P.K. Egeberg, G.R. Dickens, Thermodynamic and pore water halogen constraints on gas hydrate distribution at ODP Site 997 (Blake Ridge), Chem. Geol. 153 (1999) 53–79.

[29] R. Hesse, S.K. Frage, P.K. Egeberg, R. Matsumoto, Stable isotope studies (Cl, O, and H) of interstitial waters from Site 997, Blake Ridge Gas Hydrate Field, West Atlantic, in: C.K. Paull, R. Matsumoto, P.J. Wallace, W.P. Dillon (Eds.), Proc. ODP Sci. Res. 164 (2000) 129–137.

[30] E. Suess, M.E. Torres, G. Bohrmann, R.W. Collier, J. Greinert, P. Linke, G. Rehder, A. Trehu, K. Wallmann, G. Winckler, E. Zuleger, Gas hydrate destabilization: enhanced dewatering, benthic material turnover and large

methane plumes at the Cascadia convergent margin, Earth Planet. Sci. Lett. 170 (1999) 1–15.

[31] W. Ussler, C.K. Paull, Effects of ion exclusion and isotopic fractionation on pore water geochemistry during gas hydrate formation and decomposition, Geo-Mar. Lett. 15 (1995) 37–44.

[32] J. Greinert, Rezente submarine Mineralbildungen: Abbild geochemischer Prozesse an aktiven Fluidaustrittsstellen im Aleuten- und Cascadia-Akkretionskomplex, Ph.D. Thesis, GEOMAR Report 87, Kiel, 1999, 196 pp.

[33] K.A. Kvenvolden, M. Kastner, Gas hydrates of the peruvian outer continental margin, in: E. Suess, R. von Huene (Eds.), Proc. ODP Sci. Res. 112 (1990) p. 517.

[34] J.B. Martin, M. Kastner, P. Henry, X. Le Pichon, S. Lallement, Chemical and isotopic evidence for sources of fluids in a mud volcano field seaward of the Barbados accretionary wedge, J. Geophys. Res. 101 (1996) 20325–20345.

[35] R. Matsumoto, W.S. Borowski, Gas hydrate estimates from newly determined oxygen isotopic fractionation (α_{GH-IW}) and $\delta^{18}O$ anomalies of the interstitial waters: Leg 164, Blake Ridge, in: C.K. Paull, R. Matsumoto, P.J. Wallace, W.P. Dillon (Eds.), Proc. ODP Sci. Res. 164 (2000) 59–66.

[36] V.I. Pashkina, A.D. Esikov, Fractionation of oxygen and hydrogen isotopes at the hydrate gas forming in the sea sediments, Isotopenpraxis 26 (1990) 600–603.

[37] D.D. Coleman, J.B. Risatti, M. Schoell, Fractionation of carbon and hydrogen isotopes by methane-oxidizing bacteria, Geochim. Cosmochim. Acta 45 (1981) 1033–1037.

[38] R. Sassen, I.R. MacDonald, N.L. Guinasso, S. Joye, A.G. Requejo, S.T. Sweet, J. Alcalá-Herrera, D.A. DeFreitas, D.R. Schink, Bacterial methane oxidation in sea-floor gas-hydrate: Significance to life in extreme environments, Geology 26 (1998) 851–854.

[39] J.R. Gat, Comments on the stable isotope method in regional groundwater investigations, Water Resour. Res. 7 (1971) 980–993.

[40] M. Kastner, H. Elderfield, J.B. Martin, Fluids in convergent margins: what do we know about their composition, origin, role in diagenesis and importance for oceanic chemical fluxes, Philos. Trans. R. Soc. London A 335 (1991) 243–259.

[41] T.B. Coplen, B.B. Hanshaw, Ultrafiltration by a compacted clay membrane I: Oxygen and hydrogen isotopic fractionation, Geochim. Cosmochim. Acta 37 (1973) 2295–2310.

[42] J.M. Gieskes, P. Vrolijk, G. Blanc, Hydrogeochemistry of the Northern Barbados Accretionary Complex Transect: Ocean Drilling Project Leg 110, J. Geophys. Res. 95 (1990) 8809–8818.

[43] K.M. Brown, D.M. Saffer, B.A. Bekins, Smectite diagenesis, pore-water freshening, and fluid flow at the toe of the Nankai wedge, Earth Planet. Sci. Lett. 194 (2001) 97–109.

[44] J.C. Moore, P. Vrolijk, Fluids in accretionary prisms, Rev. Geophys. 30 (1992) 113–135.

[45] V.A. Colten-Bradley, Role of pressure in smectite dehydration - Effects on geopressure and smectite-to-illite transformation, AAPG Bull. 71 (1987) 1414–1427.

[46] R.M. Capuano, The temperature dependence of hydrogen isotope fractionation between clay minerals and water: Evidence from a geopressured system, Geochim. Cosmochim. Acta 56 (1992) 2547–2554.

[47] T.G. Fitts, K.M. Brown, Stress-induced smectite dehydration: ramifications for the patterns of freshing and fluid expulsion in the N. Barbados accretionary wedge, Earth Planet. Sci. Lett. 172 (1999) 179–197.

[48] T.A.C. Zitter, S.J. Van der Gaast, J.M. Woodside, New informations concerning clay mineral provenance in mud volcanoes, in: 36th CIESM congress, Rapp. Comm. Inter. Mer Médit. 36, Monte Carlo, 2001, 46 pp.

[49] R.A. Morton, L.S. Land, Regional variations in formation water chemistry, Frio Formation (Oligocene), Texas Gulf Coast, AAG Bull. 71 (1987) 191–206.

[50] E. Suess, G. Bohrmann, R. von Huehne, P. Linke, K. Wallmann, G. Winckler, R.A. Lutz, O. Orange, Fluid venting in the eastern Aleutian subduction zone, J. Geophys. Res. 103 (1998) 2597–2614.